GROUND MOTION TIME HISTORIES FOR THE I880 BRIDGE, OAKLAND

Prepared for the PEER Methodology Testbeds Project
by Paul Somerville and Nancy Collins
URS Corporation, Pasadena, CA.
Feb 5, 2002

Introduction

Near fault ground motions contain forward rupture directivity pulses and static ground displacements. These characteristics are described in Somerville (2002), which is posted on this website, and the way in which they are treated in the development of time histories for the I880 bridge is described below.

Site Conditions

The ground motion time histories described in this report are for free field soft rock site conditions (S_C). Testbed team members will use these time histories to generate ground motion time histories that represent surface or foundation level ground motions. These modifications need to account for the fact that the rock ground motions represent free field motions, not motions at depth. **The user must transform the strike normal and strike parallel components into longitudinal and transverse components**.

Uniform Hazard Spectra

The uniform hazard spectra for S_C site conditions (Table 1) are derived from a probabilistic seismic hazard analysis for a site in Oakland. The spectra were obtained for soil site conditions (S_D). Spectra for rock site conditions S_C were derived from the soil site spectra by multiplying the soil site spectra by the ratio of rock to soil spectra. These ratios are for the mode magnitude and distance combinations from the deaggregation of the hazard, listed in Table 2. These are magnitude 6.6, 6.8 and 7.0 earthquakes at a closest distance of 7 km using the ground motion model of Abrahamson and Silva (1997). The rock sites used in the development of these relations represent S_C site conditions (Rodriguez-Marek, 2000), and the soil sites represent S_D site conditions. The spectra contain rupture directivity effects, which were represented in the probabilistic ground motion hazard analysis using the empirical model of Somerville et al. (1997). Separate response spectra are provided for the strike-normal (SN) and strike-parallel components (SP).

Table 1. Uniform Hazard Spectra, 5% damping, at the I880 Bridge site

I880 - 50% in 50 Years				
	Rock, S_C		**Soil,** S_D	
Period	**SN**	**SP**	**SN**	**SP**
0.03	0.453	0.453	0.337	0.337
0.075	0.902	0.902	0.596	0.596
0.10	1.025	1.025	0.698	0.698
0.20	1.144	1.144	0.883	0.883
0.30	0.909	0.909	0.847	0.847
0.50	0.572	0.572	0.683	0.683
0.70	0.369	0.367	0.528	0.525
1.00	0.294	0.291	0.449	0.445
2.00	0.127	0.125	0.226	0.223
3.00	0.074	0.069	0.134	0.125
4.00	0.046	0.043	0.085	0.078

I880 - 10% in 50 Years				
	Rock, S_C		**Soil,** S_D	
Period	**SN**	**SP**	**SN**	**SP**
0.03	0.871	0.871	0.642	0.642
0.075	1.642	1.642	1.071	1.071
0.10	1.924	1.924	1.294	1.294
0.20	2.087	2.087	1.594	1.594
0.30	1.690	1.690	1.560	1.560
0.50	1.108	1.108	1.316	1.316
0.70	0.766	0.753	1.094	1.077
1.00	0.601	0.580	0.917	0.886
2.00	0.287	0.279	0.513	0.498
3.00	0.206	0.164	0.376	0.298
4.00	0.149	0.106	0.275	0.195

I880 - 2% in 50 Years				
	Rock, S_C		Soil, S_D	
Period	**SN**	**SP**	**SN**	**SP**
0.03	1.228	1.228	0.896	0.896
0.075	2.368	2.368	1.523	1.523
0.10	2.739	2.739	1.820	1.820
0.20	3.091	3.091	2.335	2.335
0.30	2.525	2.525	2.312	2.312
0.50	1.696	1.696	2.002	2.002
0.70	1.206	1.177	1.718	1.677
1.00	0.982	0.931	1.499	1.421
2.00	0.479	0.457	0.859	0.820
3.00	0.392	0.273	0.717	0.499
4.00	0.289	0.181	0.533	0.333

Deaggregation of the Hazard

The deaggregation of the hazard at a period of 1 second is given in Table 2. At all three hazard levels, the hazard is dominated by earthquakes on the Hayward fault, which is located about 7 km east of the site. The Hayward fault is a strike-slip fault that has the potential to generate earthquakes having magnitudes as large as 7. For all three hazard levels, the largest contributions come from magnitudes in the range of 6.6 to 7.0. The higher ground motions for the lower probability levels mainly reflect higher ground motion levels for the same magnitude (larger number of standard deviations above the mean), rather than larger magnitudes.

Table 2. Deaggregation of Hazard Spectra, 5% damping, Strike Parallel, Sa at 1 seconds, at the I880 Bridge Site

Hazard Level	Sa at 1 sec	M mode	R mode
50% in 50 years	0.291	6.6	7 km
10% in 50 years	0.580	6.8	7 km
2% in 50 years	0.931	7.0	7 km

Process of Selecting Ground Motion Recordings

The recordings listed in Tables 3 and 4 were selected to satisfy to the extent possible the magnitude and distance combinations listed in Table 2 for strike-slip earthquakes on S_C sites. In general, it was not easy to satisfy these requirements, and none of the sets of time histories is larger than the minimum requirement of ten. It was not possible to satisfy the distance requirement exactly, but all of the selected recordings are within about 10 km of the fault. In all but a few cases, the recordings are from sites that are classified as S_C, but in general these site classifications are not based on shear

wave velocity measurements. If there were a much larger set of recordings to choose from, it is likely that the sets of selected recordings would have less variability than the sets that are provided.

Time Histories for 50% in 50 years

The time histories used to represent the 50% in 50 year ground motions are listed in Table 3. Three of the recordings are from sites that are classified as S_D. No attempt was made to adjust these recordings for S_C site conditions. Two of the recordings are from the abutment of the Coyote Lake dam.

Time Histories for 10% in 50 years and 2% in 50 years

The time histories used to represent the 50% in 50 year ground motions are listed in Table 4. The same set of time histories is used to generate the two sets. This is justified in part by the fact that the magnitude – distance combinations that dominate the hazard in each case are the same (Table 2). However, this ignores the fact that the 2% in 50 year time histories should be drawn from larger ground motion recordings than the 10% in 50 year time histories.

Table 3. Time histories representing 50% in 50 year hazard level at the I880 Bridge

Earthquake	Mw	Station	Distance	Site	Scale	Reference
Coyote Lake, 1979/6/8	5.7	Coyote Lake Dam abutment	4.0	C	unscaled	Liu & Helmberger, 1983
		Gilroy #6	1.2	C	unscaled	
Parkfield, 1966/6/27	6.0	Temblor	4.4	C	unscaled	Cloud & Perez, 1967
		Array #5	3.7	D	unscaled	
		Array #8	8.0	D	unscaled	
Livermore, 1980/1/27	5.5	Fagundes Ranch	4.1	D	unscaled	Boatwright & Boore, 1983.
		Morgan Territory Park	8.1	C	unscaled	
Morgan Hill, 1984/4/24	6.2	Coyote Lake Dam abutment	0.1	C	unscaled	Hartzell & Heaton, 1986
		Anderson Dam Downstream	4.5	C	unscaled	
		Halls Valley	2.5	C	unscaled	

Table 4. Time histories representing 10% in 50 year and 2% in 50 year hazard levels at the I880 Bridge

Earthquake	Mw	Station	Distance	Site	Scale, 10/50	Scale, 2/50	Reference
Loma Prieta, 1989/10/17	7.0	Los Gatos Presentation Center	3.5	C	unscaled	unscaled	Wald et al., 1991
		Saratoga Aloha Ave	8.3	C	unscaled	unscaled	
		Corralitos	3.4	C	unscaled	unscaled	
		Gavilan College	9.5	C	unscaled	unscaled	
		Gilroy historic		C	unscaled	unscaled	
		Lexington Dam abutment	6.3	C	unscaled	unscaled	
Kobe, Japan, 1995/1/17	6.9	Kobe JMA	0.5	C	unscaled	unscaled	Wald, 1996
Tottori, Japan, 2000/10/6	6.6	Kofu	10.0	C	unscaled	unscaled	K-net
		Hino	1.0	C	unscaled	unscaled	Kik-net
Erzincan, Turkey, 1992/3/13	6.7	Erzincan	1.8	C*	unscaled	unscaled	EERI, 1993

There is a remarkable sparsity of appropriate recordings on rock from strike-slip California earthquakes in the magnitude range of 6.5 to 7. The recording that would nominally appear to be the best representations of a Hayward fault earthquake is the recording of the Kobe earthquake. However, the rheology of the faults that produced the Kobe earthquake may be quite different from that of the Hayward fault, which has been described by Bergmann et al., 2000.

The Kofu recording of the Tottori earthquake was obtained at a K-net site whose soil and seismic wave velocity profiles are known to bedrock at a depth of 10 km (Table 5). The Hino recording of the Tottori earthquake was obtained at a Kik-net site whose soil and seismic wave velocity profiles are known to a depth of 100 meters (Table 6). The Hino site consists of 10 meters of sand and gravel overlying weathered granite. The spectral peak at a period of about 0.7 second is interpreted as indicating strong non-linear effects. The ground motion level at the Kofu site was apparently not high enough to cause similar nonlinear effects at Kofu, whose soil also has higher shear wave velocity.

The Erzincan recording of the Erzincan earthquake was recorded on deep alluvium (EERI, 1993). It was spectrally modified to represent a rock site recording. The target spectrum for the spectral matching was obtained by scaling the recorded spectrum by the ratio of rock to soil in the Abrahamson and Silva (1997) ground motion

Table 5. Soil Profile at K-net Site Kofu (TTR007)

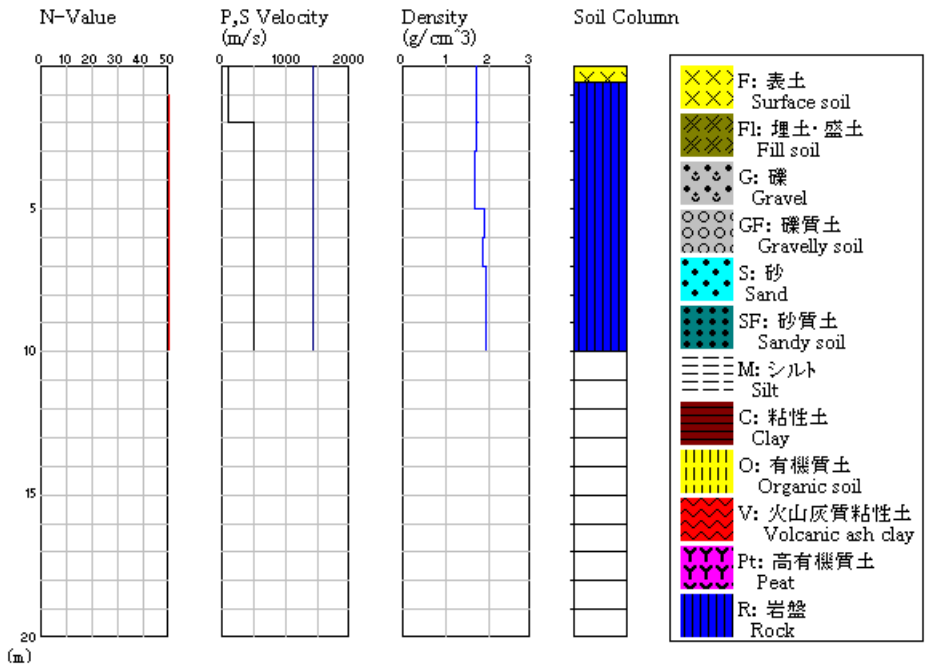

relations. The resulting response spectrum is very compatible with the uniform hazard spectrum. The rheology of the Anatolia fault on which the Erzincan earthquake occurred is considered to be potentially quite compatible with that of the Hayward fault.

The Lexington Dam record was obtained on the rock abutment of Lexington Dam. Using this recording as a representation of the input ground motions at the base of the dam, several investigators have successfully modeled the recordings from the crest of the dam (Mejia et al., 1992; Makdisi et al., 1994), implying that the abutment recording is not severely contaminated by dam interaction effects.

Representation of Near Fault Rupture Directivity Effects in the Ground Motion Recordings

The selected ground motion time histories were all recorded sufficiently close to the fault to contain rupture directivity effects. In strike-slip earthquakes, forward rupture directivity (propagation of rupture horizontally towards the recording station) produces a pulse of intermediate or long period ground motion whose particle motion is orientated in the direction normal to the strike of the fault (Somerville et al., 1997; Somerville, 1998; Somerville et al., 2000; Somerville, 2002). This pulse is manifested by a response spectrum that is larger on the strike normal component than on the strike parallel component at periods longer than about 0.5 seconds. There are indications that the period of the pulse may increase with magnitude (Somerville, 2000). If the earthquake ruptures away from the recording station, then rupture directivity effects are less pronounced. Some of the selected recordings contain strong forward rupture directivity pulses, but others do not.

Soil &Rock Condition

Station Point: HINO
Station Code: TTRH02
Location : TOTTORIKEN HINOGUN HINOCHO SHIMOKUROSAKA 1251-2
Latitude : 35 deg 14 ' 40.0 "
Longitude : 133 deg 23 ' 37.0 "
Altitude : +410m
Depth : 103.00m

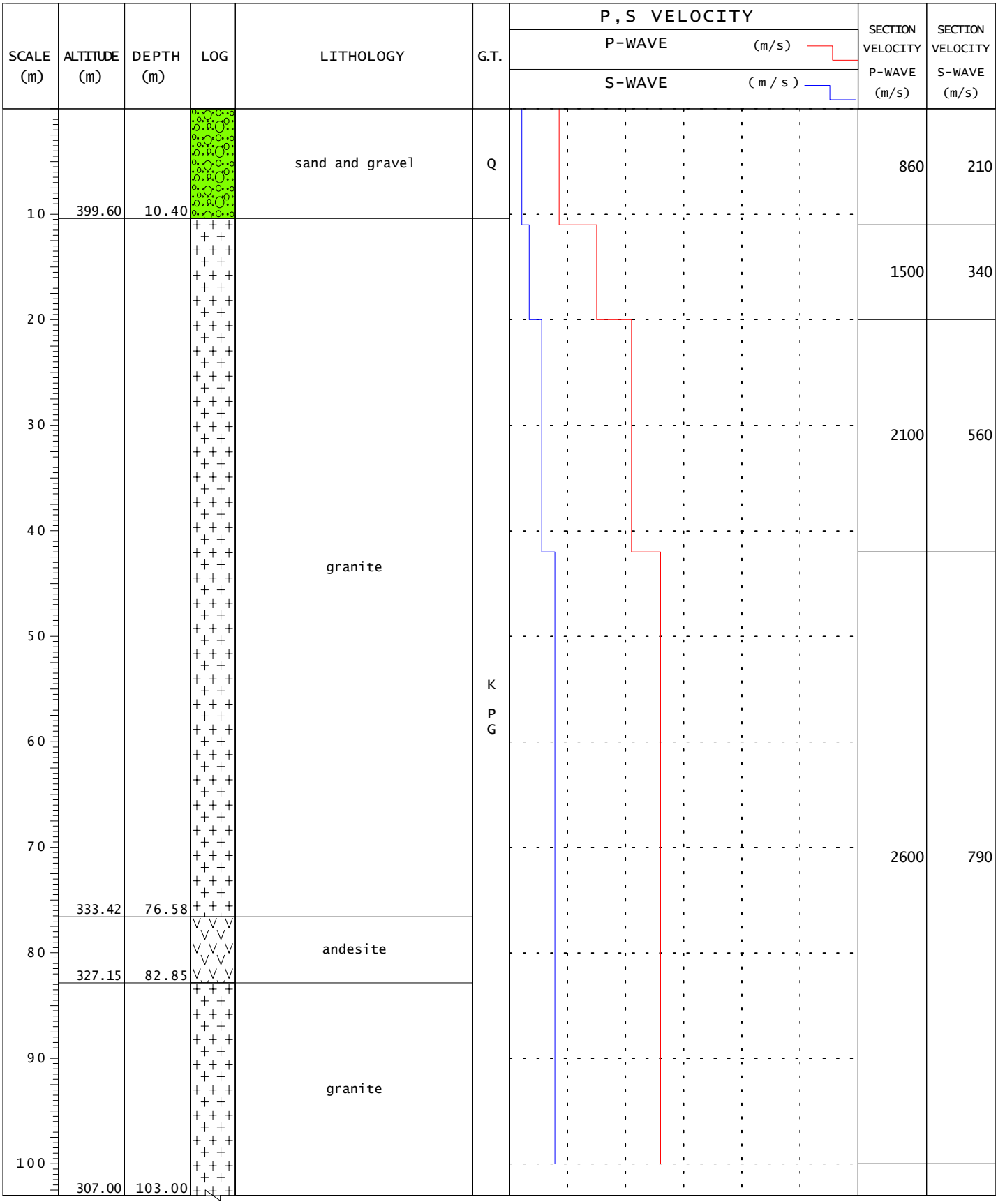

All of the recorded time histories were rotated to the strike normal and strike parallel directions. Generally, if the recording contains forward rupture directivity effects, its transverse component is expected to be larger than its longitudinal component for peak velocity and peak displacement, and for spectral accelerations having periods longer than about 0.5 seconds. This expectation is generally borne out in the recordings.

In the vicinity of the I880 Bridge, the Hayward fault has a strike of N 34 degrees west. This fixes the orientation of the two horizontal components for input into the I880 Bridge. **This orientation must not be changed**. The bridge is curved, so there is no single rotation of the time histories that would yield transverse and longitudinal components that apply to the whole length of the bridge, although roughly speaking, the strike parallel direction is transverse and the strike normal direction is longitudinal.

The user must transform the strike normal and strike parallel components into longitudinal and transverse components, after scaling them in their strike normal and strike parallel form (see below under scaling). This can be done as follows. If the axis of the structure is aligned at some angle θ to the strike of the fault, then the longitudinal and transverse time histories can be derived from the strike-normal (SN) and strike-parallel (SP) time histories using the following transformation:

$$\text{long} = SP \cos\theta + SN \sin\theta$$
$$\text{trans} = SP \sin\theta - SN \cos\theta$$

Site Effects in the Ground Motion Recordings

The shallow stiff soil conditions at the site have the potential of causing strong resonances in the ground motions. Some of the recordings contain resonances at periods shorter than 0.45 seconds that may be attributable to such effects.

Many of the recordings have response spectral amplitudes that are larger than the uniform hazard spectrum at periods longer than 0.45 seconds. In many cases, these may be attributable to forward rupture directivity effects.

In near fault recordings on soil sites, it may be difficult to separate site response effects from rupture directivity effects. As shown by Rodriguez-Marek (2000), the effect of the soil layer is generally to increase both the peak velocity and the period of the input rock motion. The amount of the increase depends on the level of the input motion, and the thickness and physical properties of the soil layer. The soil layer may thus generate effects that resemble those of near fault rupture directivity.

Scaling of the Ground Motion Recordings

The ground motion time histories have not been scaled, because a unique period for use in scaling has not been identified. Once a period has been identified, a scaling factor should be found for the strike normal component using the strike normal response spectral value. This scaling factor should then be applied to all three components of the

recording. This scaling procedure preserves the relative scaling between the three components of the recording. Consequently, the longitudinal (close to strike-normal) component will generally be larger than the transverse (close to strike-parallel) component at longer periods for many of the recordings, due to forward rupture directivity effects. The strike-normal and strike-parallel components can then be transformed into longitudinal and transverse components using the method described above.

References

Abrahamson, N.A. and W.J. Silva (1997). Empirical response spectral attenuation relations for shallow crustal earthquakes. *Seismological Research Letters* 68, 94-127.

Boatwright, J, and D.M. Boore. Analysis of the ground accelerations radiated from the 1980 Livermore Valley earthquakes for directivity and dynamic source characteristics.

Burgmann, R., D. Schmidt, R.M. Nadeau, M. d'Alessio, E. Fielding, D. Manaker, T.V. McEvilly, and M.H. Murray (2000). Earthquake potential along the Northern Hayward Fault, California. Science 289, 1178-1182.

Cloud, W.K. and V. Perez (1967). Accelerograms – Parkfield earthquake. *Bull. Seism. Soc. Am.,* **57,** 1179-1192.

Earthquake Engineering Research Institute (1993). Erzincan, Turkey Earhquake of March 13, 1992: Reconnaissance Report, Chapter 2 – Geology and Geotechnical Effects. Earthquake Spectra, Supplement to Volume 9.

Geomatrix Consultants, 2000, Geologic hazards investigation, Central campus, University of California, Berkeley, California, Appendix One, Report prepared for The Economic Benefits of a Disaster Resistant University.

Hartzell, S. H. and T. H. Heaton (1986). Rupture history of the 1984 Morgan Hill, California, earthquake from the inversion of strong motion records, *Bull. Seism. Soc. Am.*, **76,** 649- 674.

Idriss, I.M. (1991). Procedures for selecting earthquake ground motions at rock sites. Report to NIST.

K-Net website: www.k-net.bosai.go.jp

KikNet website: www.kik.bosai.go.jp

Liu, H. L. and D. V. Helmberger (1983). The near-source ground motion of the 6 August 1979 Coyote Lake, California, earthquake, *Bull. Seism. Soc. Am.*, **73**, 201-218.

Makdisi, F., C.-Y. Chang, Z.-L. Wang, and C.-M. Mok (1994). Analysis of the recorded response of Lexington Dam during various levels of ground shaking. Data Utilization Report CSMIP/94/03.

Mejia, L., J. Sun, S. Salah-Mars, Y. Moriwaki and M. Bekai (1992). Nonlinear dynamic response analysis of Lexington Dam, Proceedings of the CSMIP 1992 Conference, Sacramento, May 22, p. 10-1 to 10-14.

Rodriguez-Marek, A. (2000). Near fault seismic site response. Ph.D. Thesis, Civil Engineering, University of California, Berkeley, 451 pp.

Sadigh, K., Chang, C.Y., Egan, J.A., Makdisi, F., Youngs, R.R., 1997, Attenuation relationships for shallow crustal earthquakes based on California strong motion data, Seismological Research Letters, Vol. 68, No. 1, January.

Somerville, P.G. (2002). Characterizing near fault ground motion for the design and evaluation of bridges. Proceedings of the Third National Seismic Conference and Workshop on Bridges and Highways. *This paper is posted on the testbed website*.

Somerville, P.G. (2000). Magnitude scaling of near fault ground motions. Earthquake Engineering and Enginering Seismology, 2, 15-24.

Somerville, P.G. (1998). Development of an improved representation of near fault ground motions. Proceedings of the SMIP98 Seminar on Utilization of Strong Ground Motion Data, p. 1-20.

Somerville, P.G., A. Pitarka and N. Collins (2001). Ground motion maps that account for site effects, basin effects, duration of shaking and rupture directivity effects in the San Francisco Bay Area, Final Report to USGS, Award No. 99-HQ-GR-0030.

Somerville, P.G., H. Krawinkler and B. Alavi (2000). Development of improved ground motion representation and design procedures for near-fault ground motions. Final Report to CSMIP Data Utilization Program, Contract No. 1097-601.

Somerville, P.G., K. Irikura, R. Graves, S. Sawada, D. Wald, N. Abrahamson, Y. Iwasaki, T. Kagawa, N. Smith and A. Kowada (1999). Characterizing earthquake slip models for the prediction of strong ground motion. *Seismological Research Letters*,70, 59-80.

Somerville, P.G., N.F. Smith, R.W. Graves, and N.A. Abrahamson (1997). Modification of empirical strong ground motion attenuation relations to include the amplitude and duration effects of rupture directivity, *Seismological Research Letters* 68, 199-222.

URS Corporation (2000). Probabilistic Ground-Motion Analysis for the Central Campus. Draft report prepared for the U.C. Berkeley Seismic Guidelines Project, June 8, 2000.

Wald, D. J., D. V. Helmberger and T.H. Heaton (1991). Rupture model of the 1989 Loma Prieta earthquake from the inversion of strong motion and broadband teleseismic data, *Bull. Seism. Soc. Am.* **81**, 1540-1572.

Wald, D.J. (1996). Slip history of the 1995 Kobe, Japan, Earthquake determined from Strong Motion, Teleseismic, and Geodetic data, *J. Physics of the Earth*, **44**, 489-503.

Working Group on California Earthquake Probabilities (1999). Earthquake probabilities in the San Francisco Bay Region: 2000 to 2030 - a summary of findings. U.S. Geological Survey Open File Report 99-517.